

Granzyme B is expressed in mouse mast cells *in vivo* and *in vitro* and causes delayed cell death independent of perforin

J Pardo^{1,7}, R Wallich^{2,7}, K Ebnet³, S Iden³, H Zentgraf⁴, P Martin¹, A Ekiciler¹, A Prins⁵, A Müllbacher⁵, M Huber⁶ and MM Simon^{*,1}

Mast cells respond to pathogens and allergens by secreting a vast array of preformed and newly synthesized mediators, including enzymes, vasoactive amines, lipid mediators, cytokines and chemokines, thereby affecting innate and adaptive immune responses and pathogenesis. Here, we present evidence that skin-, but not lung-associated primary mast cells as well as *in vitro*-differentiated bone marrow-derived mast cells (BMMC) express granzyme (gzm) B, but not gzmA or perforin (perf). GzmB is associated with cytoplasmic granules of BMMC and secreted after Fc ϵ -receptor-mediated activation. BMMC from wild type but not gzmB-deficient mice cause cell death in susceptible adherent target cells, indicating that the perf-independent cytotoxicity of BMMC is executed by gzmB. Furthermore, gzmB induces a disorganization of endothelial cell–cell contacts. The data suggest that activated mast cells contribute, via secreted gzmB, to cell death, increased vascular permeability, leukocyte extravasation and subsequent inflammatory processes in affected tissues.

Cell Death and Differentiation (2007) 14, 1768–1779; doi:10.1038/sj.cdd.4402183; published online 29 June 2007

Mast cells are mainly known for their role in allergic disorders, but have recently been shown to exert many other immune functions.¹ Mast cells constitute a heterogeneous population residing in mucosal and connective tissues and are found in close association with endothelial cells (ECs) of blood vessels and nerves. Mast cell subsets are functionally distinct and their profile of expressed mediators is altered in disease states.^{1–3}

On receiving the appropriate stimuli, mast cells can release three classes of mediators: preformed granule-associated mediators, such as histamine, tryptase, chymase and other proteases; newly generated lipid mediators, that is, leukotrienes and prostaglandins; and a variety of cytokines and chemokines.^{1–3} In contrast to lipid mediators and cytokines, which have to be synthesized *de novo*, preformed granule-associated mediators can be secreted almost without delay after triggering of certain receptors.¹

Recent work on mouse has identified transcripts for the serine proteinase granzyme (gzm) B in cultured naive mast cells.⁴ However, protein expression of gzmB has not been shown. GzmB together with gzmA and perforin (perf) are key components of the lytic machinery of cytotoxic leukocytes, that is, natural killer (NK) cells and cytotoxic T lymphocytes (CTL)⁵ and are released into the immunological synapse formed between NK/CTL and their target cells.⁶ After

localization of the gzms to the cytosol and/or nucleus of target cells, gzmA and gzmB initiate alternative proteolytic pathways leading to apoptosis. These processes are strictly dependent on perf.^{5,7} However, evidence of extracellular function(s) of gzmA^{8,9} and gzmB,^{10,11} independent of perf exists. These extracellular activities of gzms are implicated in inflammation and processes of leukocyte extravasation.^{10,12,13} Both, gzmA and/or gzmB cleave extracellular proteins such as fibronectin, collagen IV, vitronectin and/or laminin.^{8,10,11} GzmB also degrades the cartilage proteoglycan aggrecan,¹⁴ induces perf-independent cell detachment and delayed cell death (anoikis) in adherent smooth muscle cells (SMCs)¹¹ and in EC.¹⁰ This occurs by remodeling of the extracellular matrix.¹⁰

Here, we report on the expression of gzmB in skin-associated and in *in vitro*-differentiated mouse mast cells and provide evidence that mast cell-derived gzmB induces cell detachment and cell death of adherent target cells.

Results

Skin- but not lung-associated mouse mast cells express gzmB *in vivo*. Histochemical analysis of skin and lung tissues from naive mice showed that skin-associated mast

¹Metschnikoff Laboratory, Max-Planck-Institut für Immunbiologie, Freiburg, Germany; ²Institute for Immunology, University Clinic Heidelberg, Heidelberg, Germany; ³Institute for Medical Biochemistry, ZMBE, University of Muenster, Muenster, Germany; ⁴German Cancer Research Center, Heidelberg, Germany; ⁵John Curtin School of Medical Research, Australian National University, Canberra, Australia and ⁶Molecular Immunology, Biology III, University of Freiburg & Max-Planck-Institut für Immunbiologie, Freiburg, Germany

*Corresponding author: MM Simon, Metschnikoff Laboratory, Max-Planck-Institut für Immunbiologie, Stübweg 51, Freiburg, Germany.

Tel: +49-761-5108-533; Fax: +49-761-5108-529, E-mail: simon@immunbio.mpg.de

⁷These authors contributed equally to this work.

Keywords: mast cells; anoikis; granzyme B

Abbreviations: B6, C57BL/6 mouse strain; BMMC, bone marrow-derived mast cell; CTL, cytotoxic T lymphocytes; EC, endothelial cell; gzm, granzyme; FHL, familial hemophagocytic lymphohistiocytosis; NK, natural killer cell; perf, perforin; RA, rheumatoid arthritis; rgzm, recombinant granzyme; SLO, streptolysin; SMC, smooth muscle cells

Received 08.11.06; revised 15.5.07; accepted 16.5.07; Edited by SJ Martin; published online 29.6.07

cells stained with both, safranin and alcian blue, whereas mast cells from lung tissue only stained with alcian blue, supporting previously published work.¹⁵ Mast cells were localized between SMCs and around small vessels in the skin (Figure 1a and b) and in subepithelial tissue layers of bronchi and bronchioles of the lung (Figure 1c). As seen in Figure 1a and b, only skin- but not lung-associated mast cells expressed gzmB, which was mainly associated with cytoplasmic granules. Tissue sections of both tissues stained with either α gzmA IgG or normal rabbit IgG were similar to untreated controls (data not shown).

In vitro-differentiated bone marrow-derived mast cells express gzmB but not gzmA or perf. Mast cells differentiated *in vitro* from bone marrow of C57BL/6 mouse strain (B6),¹⁶ termed bone marrow-derived mast cells (BMMC), consisted of greater than 95% CD117⁺ST2⁺ cells with only a minority (between 0.6 to 1%), if any, also staining for Gr-1 (data not shown), Mac-1, NK1.1, B220, CD4 or CD8 (Figure 2a). Further analysis by EM verified that the

majority of CD117⁺ST2⁺ cells are of mast cell origin (Figure 2b). When BMMC of B6 and gzmB^{-/-} mice were analyzed by FACS for intracellular expression of gzmA and gzmB proteins, all B6 BMMC (96% CD117⁺ST2⁺; Figure 3a, upper panel) specifically stained intracellularly with α gzmB- but not α gzmA-specific immune serum (IS), whereas gzmB^{-/-} BMMC gave no signal with either of the two IS (Figure 3a, lower panel).

The specificity of both IS for the respective gzm was confirmed, as before,¹⁷ by showing that the CTL line 1.3E6, but not the thymoma line, EL4, intracellularly stained for both gzms (Figure 3b, left panel) and that specific bands of the expected size of MW ~30 kDa for gzmB were found in Western blot (WB) with cell lysates from 1.3E6 and *ex vivo*-derived LCMV-immune B6 and gzmA^{-/-}, but not gzmB^{-/-} CTL, and not in EL4 cells (Figure 3b, right panel). RT-PCR analysis showed that B6 and gzmB^{-/-} BMMCs expressed transcripts specific for *Mc-cpa* with similar intensity, but only B6 BMMC contained, in addition, *gzmB*-specific mRNA (Figure 3c, left panel). Furthermore, none of the two BMMC

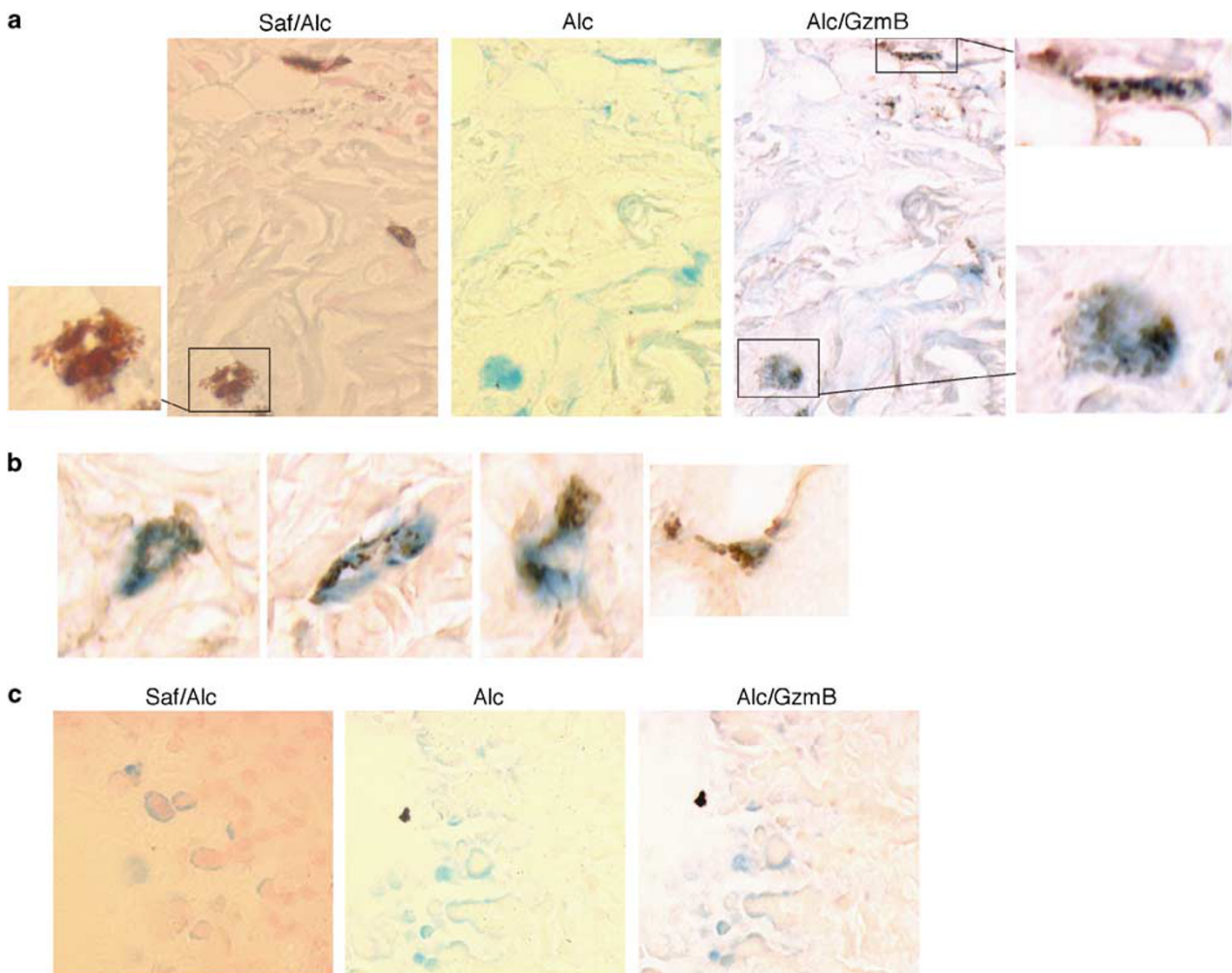


Figure 1 Mouse skin- but not lung-associated mast cells express gzmB. Tissue sections of skin and lung from naive B6 mice were stained with safranin/alcian blue (saf/alc) (a, c) or alcian blue alone (alc) (a, c), as described in Materials and methods. Consecutive sections of alcian blue-stained tissue were stained for gzmB (a, b, c) as described in Materials and methods. (a, c) Pictures of the sequential sections (saf/alc versus alc). (a) Magnifications from the respective location on the same section (alc/gzmB) are shown. (b) Different skin-associated mast cells staining for alcian blue and gzmB are shown. Original magnification: $\times 1000$

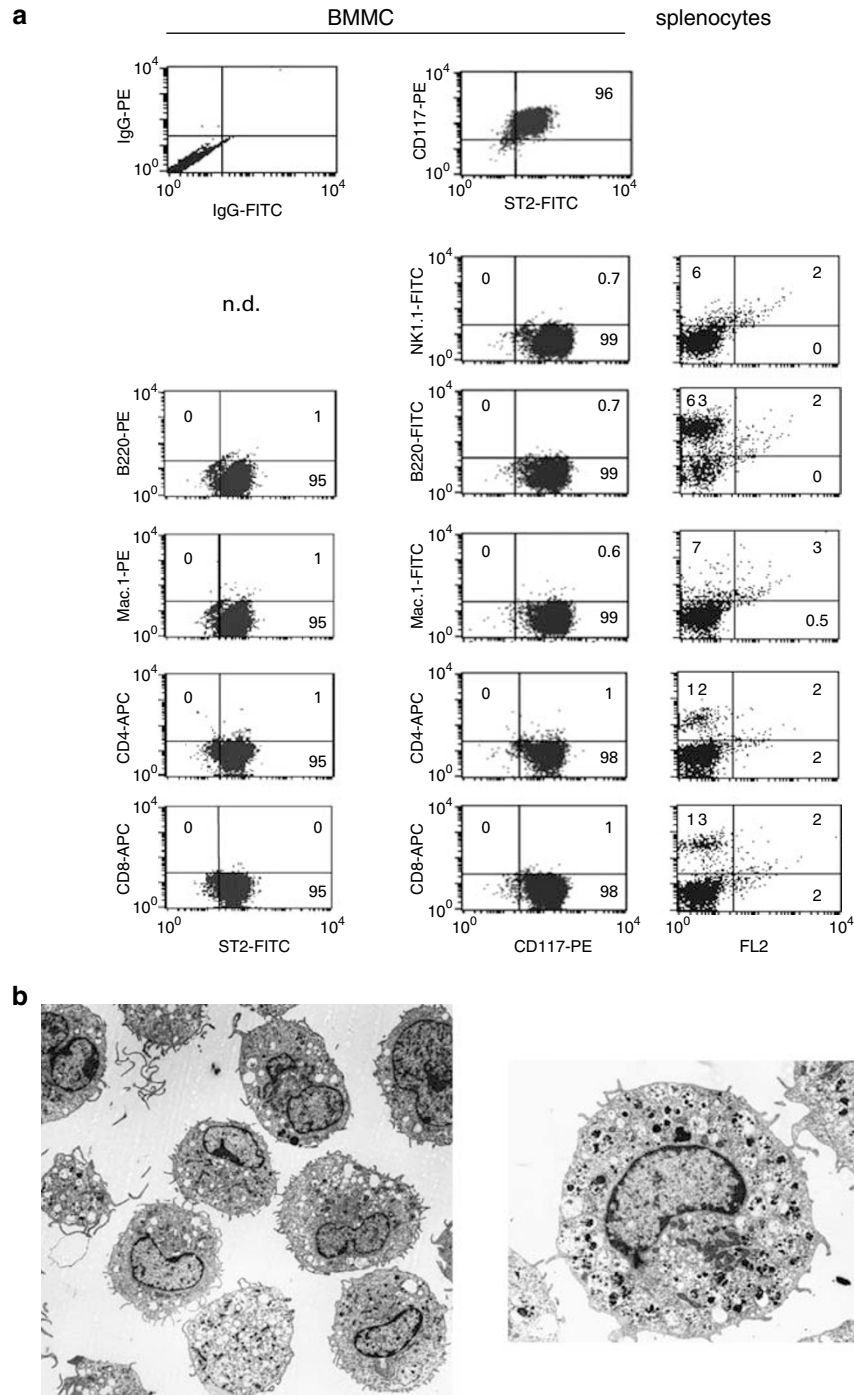


Figure 2 Phenotypic and EM analysis of mouse BMBC (a) BMBC from B6 mice were generated and analyzed for the surface markers c-kit (CD117), ST2, B220, Mac-1, NK1.1, CD8 or CD4 by FACS, as described in Materials and methods. Normal IgG (IgG-PE/IgG-FITC) was included as negative control. Numbers represent the percentage of cells in each quadrant. As positive control for the markers B220, Mac-1, NK1.1, CD8 or CD4, normal splenocytes were stained with the respective Ab. (b) Survey electron micrograph of a typical B6 BMBC population; magnification $\times 1850$ (top). A representative cell from the B6 BMBC population showing numerous vacuoles mostly filled with electron dense material; original magnification $\times 4000$ (bottom)

populations expressed *gzmA*-, *Prf-1* (Figure 3c, left panel) or any of the other *gzm*-specific mRNAs, including *gzmC*, *D*, *E*, *F*, *G*, *K* and *M* (data not shown).⁵ 1.3E6 and EL4 were negative for *Mc-cpa* mRNA and showed the expected expression patterns for *gzmA*, *gzmB* and *Prf1* transcripts

(Figure 3c, left panel).¹⁷ In addition, only B6, but not *gzmB*^{-/-} BMBC produced *gzmB*, and neither of them *gzmA* or *perF* (Figure 3c, right panel). The control cells, 1.3E6 and EL4, showed the expected banding patterns for *gzms* and *perF* proteins in WB. Confocal microscopy revealed a granular-like

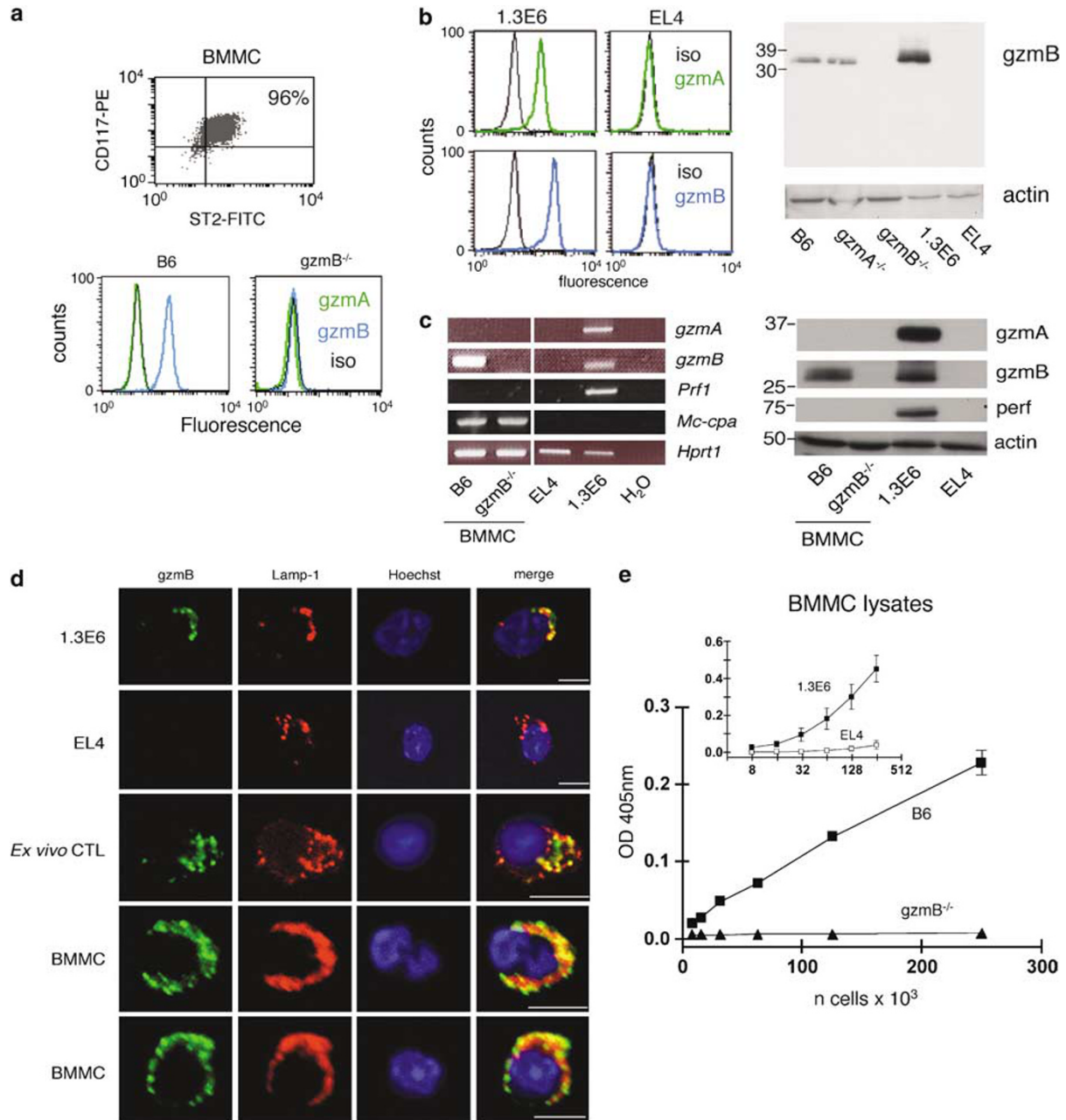


Figure 3 BMMC express gzmB, but not gzmA and perf in cytoplasmic granules. (a) BMMC from B6 and *gzmB*^{-/-} mice were generated and analyzed for intracellular gzmA and gzmB expression by FACS, using α gzmA or α gzmB IS, as described in Materials and methods. As controls, the T cell lines 1.3E6 (CTL, expressing both gzmA and gzmB) and EL4 (thymoma, negative control) were used (b, left panel). The specificity of the α gzmA and α gzmB IS was verified by WB, using cell extracts from 1.3E6, EL4 or from *ex vivo*-derived LCMV-immune CTL from B6, *gzmA*^{-/-} or *gzmB*^{-/-} mice (b, right panel) as indicated. (c) RT-PCR (left panel) and WB (right panel) analyses were performed with mRNA or cell lysates, respectively, from 1.3E6, EL4 and B6 and *gzmB*^{-/-} BMMC, using specific primer pairs for *Prf1*, *gzmA*, *gzmB* or *Mc-cpa* as well as the α gzmA and α gzmB IS and the α perf mAb, as described in Materials and methods. As controls, *Hprt1* was used for RT-PCR and actin for WB. (d) Confocal images showing B6 BMMC, 1.3E6, *ex vivo*-derived LCMV-immune CTL and EL4 stained with α gzmB IS (green) and Lamp-1 (red). Cells were mounted in a drop of Fluoromount G containing 10 μ g/ml Hoechst 33342 and fluorescence images were taken at room temperature on a confocal microscope (TCS SP2; Leica) using a $\times 40$ objective (HCX PL APO CS; Leica), NA 1.25, immersion oil and confocal software (version 2.61; all Leica). Photoshop CS2 software (Adobe) was used for minor adjustments to contrast. Bars 6 μ m. Data shown are representative of at least three independent experiments. (e) Cell lysates of B6 and *gzmB*^{-/-} BMMC were tested for gzmB activity on the respective chromogenic substrate; cell lysates of 1.3E6 or EL4 served as controls (inset). Data are given as mean \pm S.E.M. of three independent experiments

staining pattern of B6 BMMC, with gzmB and LAMP-1, a prominent lysosomal membrane marker¹⁸ colocalizing to great extent in these lysosomal compartments (Figure 3d). This suggests that in BMMC, gzmB mainly accumulates in

cytosolic granules, similar to 1.3E6 CTL and *ex vivo*-derived LCMV-immune CTL, where the majority of LAMP-1-positive organelles also expressed gzmB (Figure 3d).¹⁹ The finding that B6, but not *gzmB*^{-/-}, mast cell lysates were able to cleave

a gzmB-specific chromogenic substrate (Figure 3e) indicates that in lysates from mouse BMMC, gzmB is enzymatically active.

Mouse BMMC secrete gzmB upon antigen-mediated crosslinking of the Fc ϵ R1. Next, it was tested whether gzmB is secreted by BMMC upon Fc ϵ R1-mediated degranulation, including the granule marker, β -hexosaminidase.²⁰ B6 or gzmB^{-/-} BMMC were loaded with DNP-

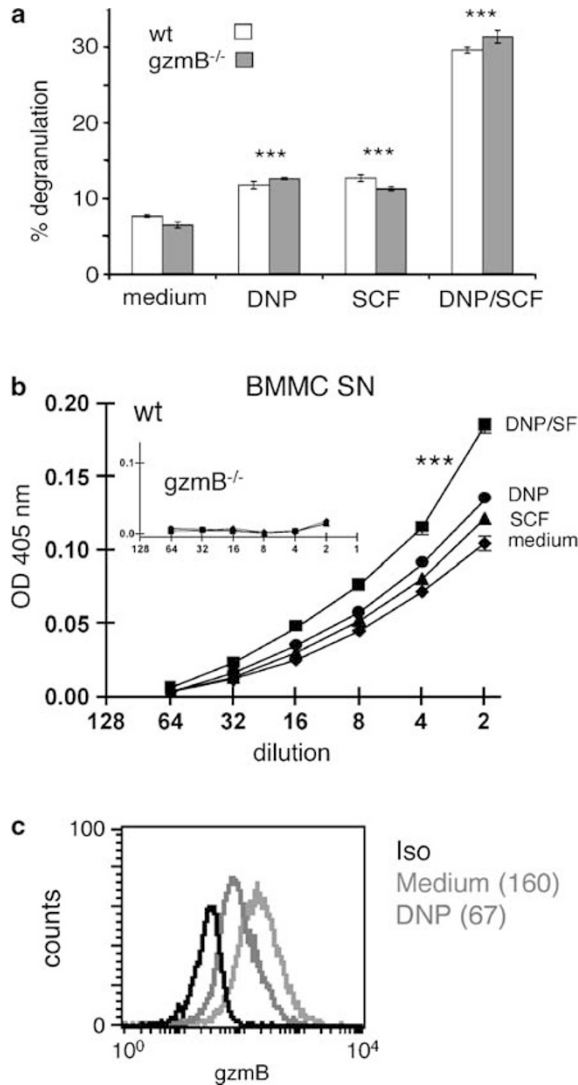


Figure 4 BMMC-associated gzmB is enzymatically active and secreted upon Fc ϵ R1-mediated activation (a, b) B6 and gzmB^{-/-} BMMC were preloaded with DNP-specific IgE Ab and subsequently challenged with either DNP-HSA (DNP), SCF or a mixture thereof for 30 min. Mock-treated (medium) B6 BMMC served as controls. BMMC SNs were tested for β -hexosaminidase (a) or gzmB activity (b). Data are given as mean \pm S.E.M. of two independent experiments. (a) ***Significantly different analyzed by 2 way ANOVA with Bonferroni posttest by comparing every experimental with control groups. (b) ***Significantly different ($P < 0.001$) comparing every treatment with medium. (c) Mock-treated or -challenged (DNP-HSA; 30 min) IgE-preloaded B6 BMMC were analyzed for intracellular gzmB by FACS (numbers in parenthesis indicate the mean intensity of gzmB-related fluorescence). A representative experiment of three independent experiments is shown

reactive IgE and stimulated with either DNP-HSA, SCF or both for 30 min. Similar high levels of β -hexosaminidase, substantially exceeding those of controls (no stimulus), were secreted from both B6 or gzmB^{-/-} BMMC, when challenged with both DNP-HSA and SCF (Figure 4a). As expected,²¹ less β -hexosaminidase was released from both BMMC populations in response to either SCF or DNP alone (Figure 4a). When challenged under similar conditions, only B6, but not gzmB^{-/-} BMMC secreted enzymatically active gzmB (Figure 4b). The amount of secreted gzmB was highest in B6 BMMC incubated with a mixture of DNP-HSA and SCF, intermediate with DNP-HSA and lowest with SCF. Furthermore, FACS analysis showed that gzmB-related mean fluorescence was considerably reduced in DNP-HSA-stimulated (67), as compared to mock-treated (160) BMMC (Figure 4c).

GzmB-induced detachment of adherent mouse embryonic fibroblasts leads to anoikis. To examine possible extracellular function(s) of BMMC-derived gzmB on adherent bystander cells and to establish optimal conditions, B6 mouse embryonic fibroblasts (MEFs) were first exposed to increasing amounts of active recombinant mouse gzmB (rgzmB). A dose-dependent change of B6 MEF morphology (rounding up) was observed after 4 h (Figure 5a; gzmB, streptolysin (SLO)), which was accompanied by a loss of cell adherence. However, even at 20 μ g/ml rgzmB, apoptotic morphology and/or cell death of MEFs (regrowth) were rarely seen (Figure 5b, upper panel). Inactive recombinant gzmB (pro-gzmB) had no effect on adherence (4 h; Figure 5a) or viability (Figure 5b) of MEFs.

When MEFs were exposed to increasing amounts of rgzmB in the presence of sublytic doses of SLO (4 h), the dose-dependent detachment (not detectable below 2 μ g/ml rgzmB, data not shown) and rounding up of MEFs was much faster and more pronounced compared to MEFs treated solely with rgzmB and associated with typical apoptotic morphology (Figure 5a). The marked induction of cell death ($\sim 50\%$, compared to untreated control) was further verified by comparing regrowth of rgzmB (20 μ g/ml) plus SLO-treated *versus* control MEFs (Figure 5b). Neither SLO alone nor SLO in the presence of pro-gzmB had any effect on MEFs (Figure 5a, b).

Treatment of MEFs with 5–20 μ g/ml rgzmB for 24 h led to a dose-dependent change in their morphology (Figure 5c) and substantial cell death at 20 μ g/ml, but not at 5–10 μ g/ml of rgzmB (Figure 5d). Incubation with pro-gzmB had no effect on MEFs morphology or viability (Figure 5c and d, upper panels). In contrast, cell death of the non-adherent EL4 cell (regrowth) only occurred in response to both rgzmB and SLO, but neither to rgzmB or SLO alone nor to pro-gzmB plus SLO under these conditions (Figure 5d, lower panel). This suggests that cell death of MEFs occurring after long-term treatment with rgzmB is not induced directly, but rather as a consequence of cell detachment from the proteolytically degraded extracellular matrix.

To assess if mast cell-derived native gzmB has similar extracellular functions as the recombinant protein, MEFs were incubated for 20 h with serial dilutions of SN (1:2 to 1:16) from IgE-preloaded and DNP-HSA-stimulated (30 min)

BMMC (Figure 6a). The gzmB-related proteolytic activity present in BMMC SN corresponded to $\sim 2\mu\text{g/ml}$ of rgzmB (Figure 6b). As for the latter, a dose-dependent effect of BMMC SN was seen on the morphology and detachment of MEFs, which was most pronounced at the highest concentration of SN and inhibitable by the gzmB-specific inhibitor, AAD-cmk (Figure 6a). SN from either gzmB^{-/-} or control BMMC (mock-treated) did not have any effect. However, as expected from the results obtained with 2.5–5 $\mu\text{g/ml}$ rgzmB (24 h; Figure 5c and d), induction of detachment and rounding up of MEFs by up to 2 $\mu\text{g/ml}$ of native gzmB (as calculated in mast cell SN) was not associated with cell death (data not shown).

BMMC from B6, but not gzmB^{-/-} mice induce cell death in MEFs. Next, B6 and gzmB^{-/-} BMMCs were preloaded with anti-DNP IgE and incubated for 20 h with either the DNP-coated adherent MEFs or non-adherent EL4 cells; the viability of target cells was monitored by recultivation (Supplementary Figure 1a and b). Only B6, but not gzmB^{-/-} BMMCs showed a significant and dose-dependent induction of cell death of MEFs (Figure 7a), but did not induce any cell death of EL4 (Figure 7b), suggesting that gzmB is the prominent cytotoxic effector molecule.

A similar effect was observed when *ex vivo*-enriched LCMV-immune CTL⁷ from mice expressing only gzmB, but not perf and/or gzmA (perfxgzmA^{-/-}), were co-cultured with adherent cells (MC.Fas^{-/-}, to exclude Fas-mediated toxicity) for prolonged periods (20 h). As shown in Figure 7c, perfxgzmA^{-/-} CTL expressing only gzmB, but not perfxgzmAxB^{-/-} CTL, lacking in addition gzmB (Supplementary Figure 1d), showed a significant dose-dependent induction of cell death of MC.Fas^{-/-} cells (regrowth; Supplementary Figure 1c, for control). As expected, B6 CTL, which express the whole cytolytic armory, including perf and both gzms (Supplementary Figure 1d), killed the majority of MC.Fas^{-/-} cells under these conditions (Figure 7c).

GzmB induces a disorganization of endothelial cell–cell contacts. To assess the possibility of mast cell-released gzmB affecting endothelial cell-to-cell contacts, bEnd5 EC were treated with various concentrations of rgzmB and stained with antibodies binding VE-cadherin. In untreated EC, VE-cadherin showed a linear staining pattern at cell-to-cell contacts (Figure 8a). Treatment with TNF- α and IFN- γ resulted in morphological changes into elongated, spindle-like shapes of EC, as described previously (Figure 8a).²² Treatment with rgzmB (20 $\mu\text{g/ml}$) resulted in disruption of cell-to-cell contacts and the appearance of multiple gaps in the monolayer (Figure 8a, right panel). A more detailed inspection of areas of cell-to-cell contact revealed that treatment with rgzmB, but not pro-gzmB, at 3 $\mu\text{g/ml}$ resulted in a fragmented staining pattern for VE-cadherin (Figure 8b). At lower concentrations of rgzmB (0.3 $\mu\text{g/ml}$), VE-cadherin fragmentation was less severe and similar to patterns observed with pro-gzmB. At higher concentrations of rgzmB (20 $\mu\text{g/ml}$), cell contacts appeared completely disorganized (Figure 8b, right panels). Furthermore, gzmB-treated bEnd.5 EC were stained with Ab against PECAM-1 and JAM-A, both of which are localized at sites of cell-to-cell contacts of EC,²³ as well as for ZO-1, a cytoplasmic protein

localized at tight junctions. Treatment of EC with 3 $\mu\text{g/ml}$ rgzmB resulted in a reduced staining as well as in a fragmented staining pattern for PECAM-1, JAM-A and ZO-1 (Figure 8c), without disturbing the integrity of the endothelial monolayer, as indicated by phase contrast microscopy (Supplementary Figure 2). The data suggest that mast cells affect endothelial cell–cell contacts via secreted gzmB thereby facilitating the recruitment of circulating leukocytes.

Discussion

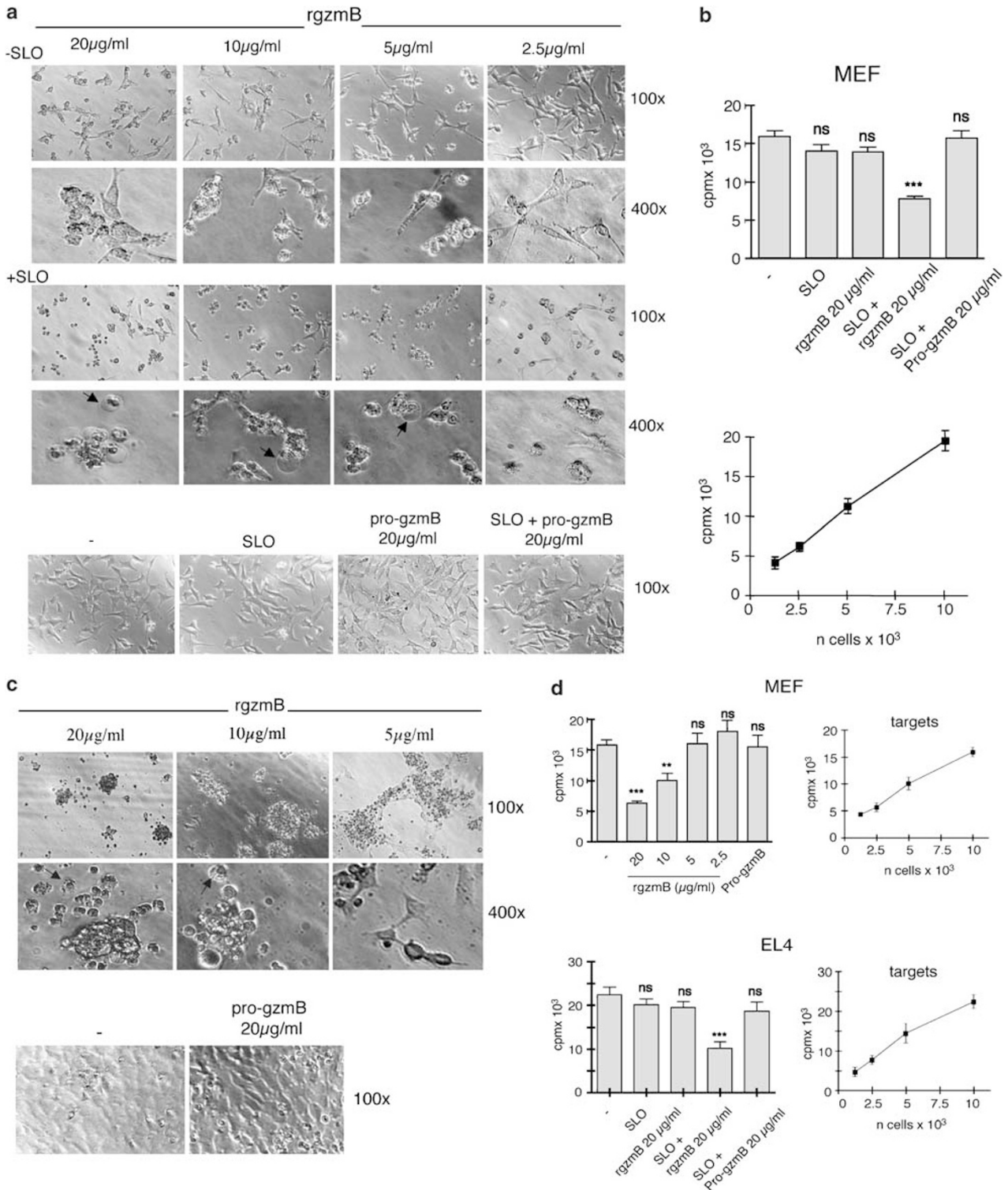
Here, we show for the first time that mouse mast cells produce gzmB, but not gzmA or perf *in vivo* as well as upon their differentiation from bone marrow cells (BMMC) *in vitro*. GzmB is associated in the lysosomal compartments of BMMC, and released in its enzymatically active form, together with other granule components, upon ligation of the receptors Fc ϵ R1 and/or c-kit. BMMC from B6, but not gzmB^{-/-} BMMC induced cell detachment and anoikis in anchorage-dependent MEF, suggesting a critical role of gzmB in this type of perf-independent killing. Although the usage of DNP to target BMMC to MEF via Fc ϵ R1 in this model is artificial, it may reflect *in vivo* situations in which crosslinking of mast cell-bound IgE Ab via antigen leads to rapid degranulation. We believe it is not unreasonable to assume that similar signaling pathways may be activated *in vivo* and lead to gzmB-mediated effector functions of mast cells in biologically relevant situations. Also, rgzmB induces morphological changes in endothelioma cells, including a fragmented staining pattern of adhesion molecules, implicating mast cell-derived gzmB in the regulation of EC contact integrity. Therefore, gzmB of mast cells might influence not only the recruitment of leukocytes during inflammatory processes associated with protective, but also pathological immune responses.

Immunohistological staining revealed that gzmB is expressed in skin- but not lung-associated mast cells from naive mice. These observations are not surprising, in particular, in connection with recent reports showing that different environmental stimuli can determine quantity, distribution and phenotype of mast cells at selected tissue sites.¹ The data presented in Figure 1 showing differential staining patterns observed with skin- versus lung-associated mast cells when using safranin and alcian blue support this contention. It is known that heparin-containing connective tissue mouse mast cells stain with both reagents, whereas the chondroitin sulfate-containing mucosal mast cells are only stained by alcian blue.¹⁵ Although both skin and lung tissue are primary target sites for host/pathogen contact, our data suggest that the mast cell phenotype found in diverse tissues, including gzmB expression, is determined by multiple factors, including physiological, inflammatory and microbial ones.

In BMMC, gzmB is associated with secretory lysosomes, that is, cytoplasmic granules, similar to that seen in CTL/NK (Figure 3).⁵ We found that gzmB colocalizes, primarily, with Lamp-1-positive (lysosomal marker)¹⁸ vesicles of BMMC and is secreted upon Fc ϵ R1/c-kit-mediated activation. This suggests that processing and assortment of gzmB to the

cytoplasmic granules, including its storage in a complex with the proteoglycan serglycin, occurs similar to that observed in CTL/NK cells.²⁴ This interpretation is supported by the finding that mast cell proteases are also stored as active enzymes in lysosomal compartments^{25,26} and that the mast cell tryptase, mMCP-6, accumulates in and is released from granules in association with serglycin.²⁷

In contrast to our data with BMDC, neoplastic human mast cells may acquire a cytolytic effector profile through combined granzyme B plus perforin expression upon activation with PMA and ionomycin (J. A. Kummer, abstract 035, *Apoptosis and Immunity* 2005, Palm Cove, Australia). It is not clear if the differential production of perforin in human versus mouse mast cells is due to the distinct activation protocols or due to variant



transcriptional regulatory events occurring in these two species. However, we cannot exclude the possibility that mouse mast cells may express *perf* in addition to *gzmb* under different conditions. BMMC, unlike CTL/NK cells, also did not express *gzmA*. It is possible that the tryptase, mMCP-6, with similar substrate specificity to that of *gzmA*, but distinct from *gzmb*,^{8,27} may substitute for *gzmA* in mast cell-induced biological processes. Thus, mMCP-6 and *gzmb* not only may execute differing nonredundant extracellular processes reminiscent of *gzmA* and *gzmb* from CTL/NK cells,^{8–10} but may also act in concert with *gzmb* on the same substrates, such as fibronectin, although with distinct cleavage specificities.^{8,10,28}

Activated BMMC from B6 but not *gzmb*^{-/-} mice caused cell death in adherent MEFs (Figure 7a), but not anchorage-independent EL4 cells (Figure 7b). This implicates *gzmb* in *perf*-independent cytolysis (anoikis).¹⁰ Recombinant and native human *gzmb* cleaves the extracellular matrix proteins, vitronectin, fibronectin and laminin, resulting in cell detachment and cell death of adherent targets, including inhibition of tumor cell spreading, migration and invasion.¹⁰ Thus, BMMC may induce anoikis, in susceptible targets, indirectly, by *gzmb*-mediated degradation of extracellular matrix proteins. That *gzmb*^{-/-} BMMC lack this selective function and that B6 BMMC do not express *gzms* A, C, D, E, F, G, K and/or M (Figure 3 and data not shown), supports this assumption. However, the contribution of other proteases, like mMCP-6, known to promote proteolytic degradation of fibronectin, with a cleavage specificity similar to *gzmA*, but distinct from *gzmb*,^{8,10,28} in these processes can not be formally excluded.

We also observed that virus immune CTL from *perfxgzmA*^{-/-} mice, which express *gzmb* but lack *gzmA* and *perf*, but not CTL from *perfxgzmAxB*^{-/-} mice, which lack *perf* and both *gzms*, are able to induce anoikis in adherent cells (Figure 7c, d) like BMMC. This suggests that NK/CTL also can induce anoikis in susceptible target cells, solely via *gzmb* and independent of *perf*. This may be explanatory for understanding the immune status of *perf* deficient individuals, such as patients with familial hemophagocytic lymphohistiocytosis (FHL).²⁹ It could be expected that FHL patients have residual NK/CTL-associated cytolytic potential and normal mast cell functions.

Mast cells are known to seed in close proximity to EC of blood vessels³⁰ and may directly act on EC and SMC, via secreted factors, including pro-inflammatory cytokines and chemokines.^{30–32} The observation that BMMC secrete *gzmb* and that *rgzmb* induces disintegration of EC-cell-cell contacts

at concentrations where gross morphological changes and EC detachment are not yet observed (3 µg/ml), may indicate that mast cell-derived *gzmb* contributes to the recruitment of leukocytes by facilitating their transendothelial migration.³³ Evidence that intraperitoneal administration of mMCP-6 results in neutrophil infiltration into the peritoneum²⁷ supports the idea of a general role for mast cell-derived proteases in leukocyte recruitment.

Most probably, *gzmb* acts on EC indirectly by cleaving ECM proteins, like fibronectin, vitronectin or laminin.¹⁰ In fact, proteolysis of ECM proteins affects integrin-mediated cell-matrix adhesion leading to subsequent cell detachment and death.³⁴ Thus, the previous finding that integrin-mediated signaling directly influences VE-cadherin-based adherens junctions³⁵ suggests a potential mechanism by which *gzmb* influences cell-cell contact integrity.

As observed previously by Buzza and Choy,^{10,36} we found extensive EC detachment at high *gzmb* concentrations (20 µg/ml) evident by multiple gaps in the endothelial monolayer. Thus, mast cell-derived *gzmb* may be responsible for cell detachment of EC, leading to their death, a feature seen in the pathogenesis of atherosclerosis.³⁷ In fact, atherosclerotic lesions in human coronary arteries have been shown to contain elevated numbers of mast cells³⁸ and an increased severity and cell death in advanced atherosclerotic lesions was associated with a presence of *gzmb*.³⁹ Furthermore, mast cell-derived *gzmb* may also contribute to vasculitis by inducing cell death in SMC, as reported.¹¹ However, only testing of atherosclerosis development in *gzmb*-deficient mice may provide evidence for the role of mast cell-derived *gzmb* in vascular diseases *in vivo*.

Mast cells have been implicated in the control of bacterial and viral infections,^{31,32} immunosurveillance, in disease progression^{1,3,30} and, more recently, as intermediaries in regulatory T cell tolerance.⁴⁰ However, the role *gzmb* may play in any of these processes is unknown. Recent evidence implicates mast cell-derived *gzmb* in the inhibition of tumorigenesis.^{1,3,10} Mast cell-secreted *gzmb* may also assist in the control of virus infections by either cleaving viral surface proteins critical for host cell entry,¹⁰ or by inducing anoikis in *gzmb*-susceptible virus-infected target cells. Mast cell migration and accumulation at sites of viral infections supports this contention.³⁰

The presence of mast cells and *gzmb*-positive cells at the invasive front of the synovium and elevated levels of *gzmb* in serum and synovial fluids is a hallmark of patients with active

Figure 5 *rgzmb* induces cell death in fibroblasts via cell detachment. (a, b) MEFs were plated before treatment (triplicates) with the indicated amounts of *rgzmb* or *pro-gzmb* in the absence or presence of a sublytic dose of SLO (0.5 µg/ml) for 4 h or were left untreated (medium). Representative microscopic images were taken from corresponding wells (a). Cell survival was monitored by recultivating MEFs and determination of ³H-thymidine incorporation as described in Materials and methods (b, upper panel). Percentage of cell death was calculated from log₂ titration curve of untreated MEFs (b, lower panel). Data are given as mean ± S.E.M. of three independent experiments performed by triplicate. ***Significantly different, *P* = 0.0001. ns, not significant. (c, d) MEFs were plated before treatment with the indicated amounts of *rgzmb* and/or *pro-gzmb* for 24 h (triplicates) and analyzed as in (a, b). In addition, non-adherent EL4 cells were treated with the indicated amounts of *rgzmb* or *pro-gzmb* in the absence or presence of a sublytic dose of SLO (0.5 µg/ml) for 24 h (d, lower panels). Cell survival was monitored by recultivating treated EL4 cells and determination of ³H-thymidine incorporation. Percentage of cell death was calculated from log₂ titration curve of untreated EL4 cells (d, lower panels). Data are given as mean ± S.E.M. of three independent experiments for MEF and two for EL4 (triplicates). (b) ***, ** significantly different, *P* < 0.0001 or 0.0011, respectively for MEF and ***, *P* = 0.0003 for EL4. ns, not significant. Analyzed by unpaired two-tailed *t*-test comparing medium with treated cells. Images were taken at room temperature using a Zeiss Axiovert 10 microscope, a Zeiss AxioCam as analysis camera, and Zeiss Vision 3.1.0.0 as software (Carl Zeiss, Jena, Germany). The objective used was a Zeiss ACHROSTIGMAT, with original magnification × 100 (NA 0.25) or × 320 (NA 0.4). Photoshop CS2 software (Adobe) was used for minor adjustments to contrast. Arrows indicate apoptotic- (a) or non apoptotic- (c) like dead cells

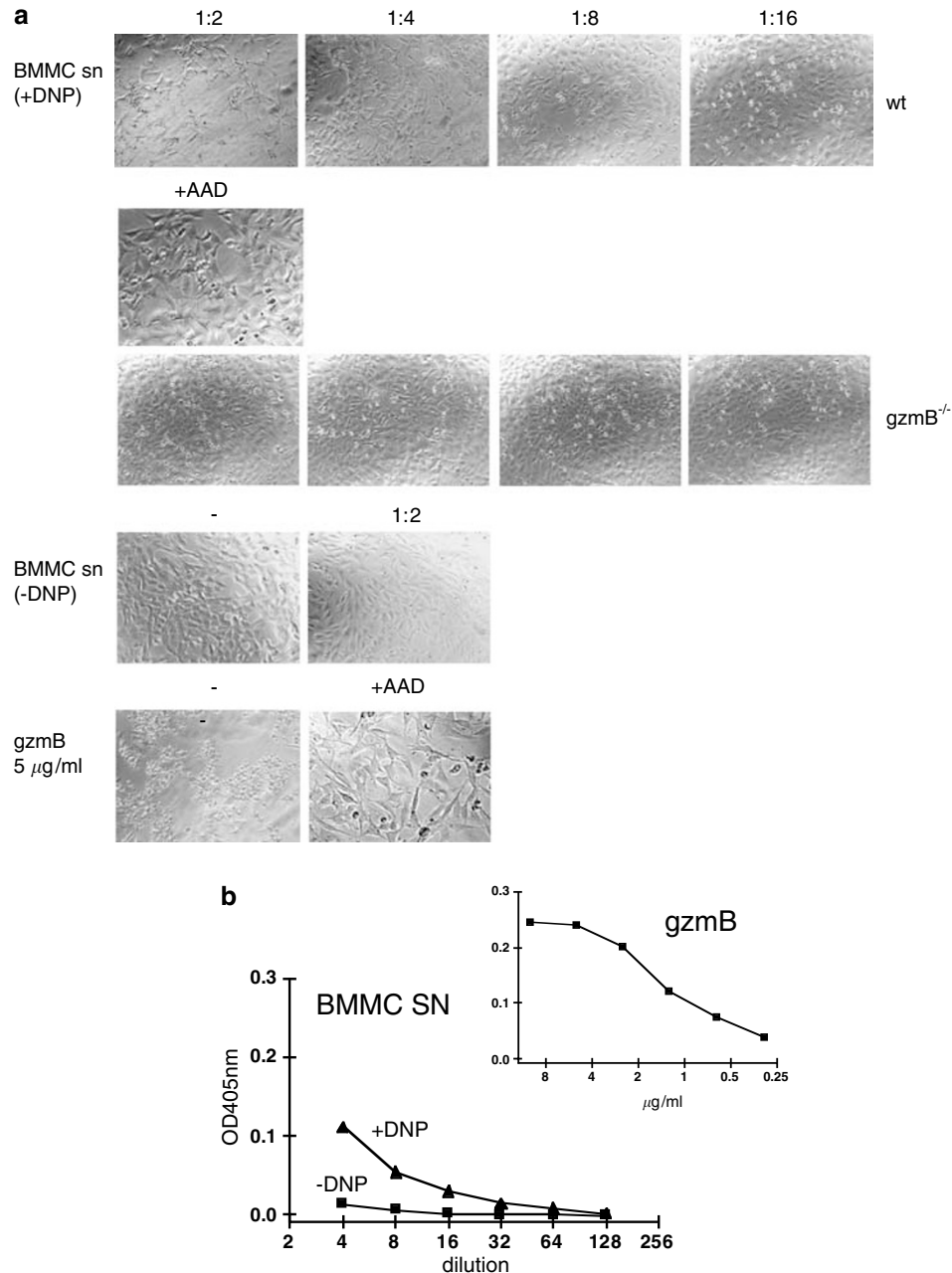


Figure 6 Supernatants of activated mast cells induce cell detachment. BMMCs from B6 or $gzmB^{-/-}$ mice, previously loaded with DNP-specific IgE, were incubated in the presence or absence of DNP-HSA for 30 min and SN were collected. (a) Attached MEFs were incubated with the indicated dilutions of SN from DNP-HSA- or mock-treated BMMC or with 5 μ g/ml rgzmB for 20 h. To inhibit the enzymatic activity of gzmB, SN of DNP-HSA-treated B6 BMMC (1 : 2 dil) and rgzmB were in addition incubated with AAD-cmk (100 μ M) for 30 min before usage. Representative microscopic images were taken from corresponding wells as described in Figure 3 (original magnification \times 100). (b) GzmB activity was tested in SN as described in Figure 2. rGzmB served as control. Data are given as mean \pm S.E.M. of two independent experiments

rheumatoid arthritis (RA).^{13,41,42} The finding of degranulated mast cells in joint tissue of mice with experimentally induced erosive synovitis and the observation that two strains of mice deficient in mast cells were resistant to the development of this type of joint inflammation⁴³ points to a likely role of mast cells in the pathogenesis of inflammatory arthritides, including RA.⁴⁴ Thus, mast cell-derived gzmB may contribute, together with other granule-associated effector molecules and mediators, to the pathogenic mechanisms of joint destruction by

facilitating recruitment of leukocytes from the circulation,^{31,32} degrading cartilage proteoglycan¹⁴ and/or by killing synovial membrane lining cells, most probably via anoikis.¹¹

Materials and Methods

Flow cytometry. Cell populations were analyzed for cell surface marker expression and/or intracellular expression of gzmA and gzmB by FACS as described previously.¹⁷ Abs are described in Supplementary material.

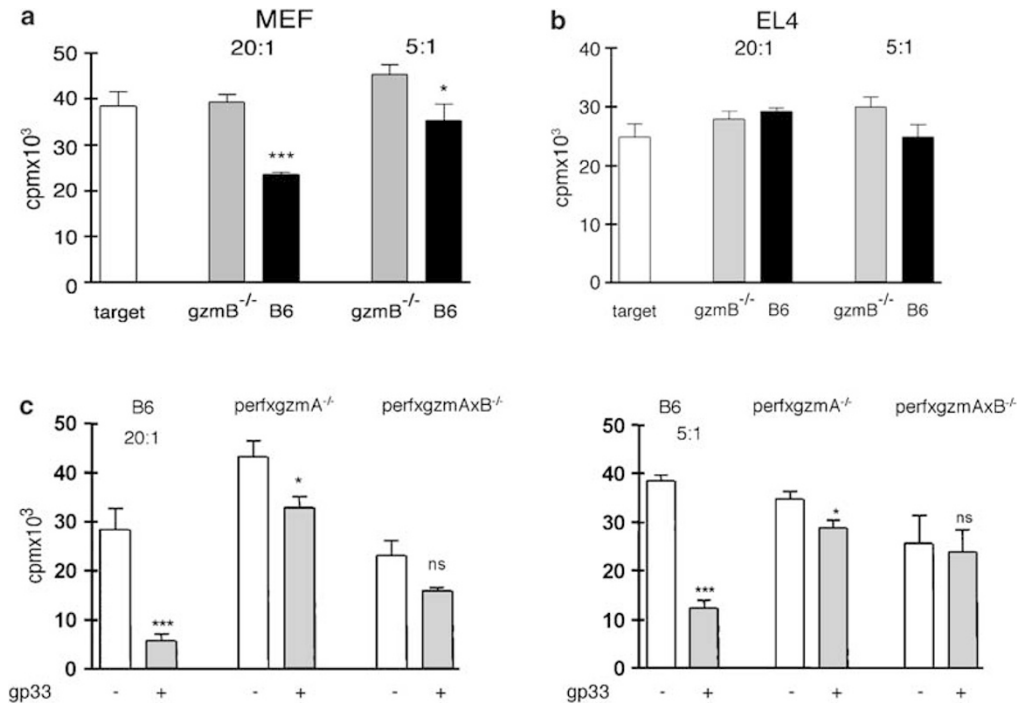


Figure 7 Intact mast cells from B6, but not from *gzmB*^{-/-} mice are able to kill MEF. BMBCs were generated from B6 or *gzmB*^{-/-} mice and incubated in triplicates with DNP-labeled MEF (a) or EL4 (b) at indicated effector : target ratios for 20 h as described in Materials and methods. Survival of target cells was analyzed by ³H-thymidine incorporation as described in Materials and methods. Data are given as mean ± S.E.M. of two independent experiments performed by triplicate. ***, * significantly different, *P* < 0.0001 or *P* = 0.035, respectively. ns, not significant. Analyzed by unpaired two-tailed *t*-test comparing wt with *gzmB*^{-/-}. When comparing effector : target ratios of 5 : 1 and 20 : 1, significant differences are only found for wt (*P* = 0.008), but not for *gzmB*^{-/-} (*P* = 0.053) BMBC. Analyzed by unpaired two-tailed *t*-test. (c) *Ex vivo*-derived LCMV-immune CTL from B6, *perfxgzmA*^{-/-} or *perfxgzmAxB*^{-/-} mice were generated as described previously⁷ and incubated with MCFas^{-/-} for 20 h with (+) or without (-) gp33 peptide, at effector : target ratios of 20 : 1 (left panel) and 5 : 1 (right panel). Survival of target cells was analyzed by ³H-thymidine incorporation as described previously.¹ Data are given as mean ± S.E.M. of two independent experiments performed by triplicate. Ratio 20 : 1, ***, * significantly different, *P* = 0.0004 or *P* = 0.0304, respectively. ns, not significant. Ratio 5 : 1, ***, * significantly different, *P* < 0.0001 or *P* = 0.0262, respectively. ns, not significant. Analyzed by unpaired two-tailed *t*-test comparing -gp33 with + gp33

Western blot analysis. Intracellular *gzmA*, *gzmB*, *perf* and *actin* were determined in cell lysates by WB under reducing conditions, as described previously.¹⁷ Abs are described in Supplementary material.

Probing for mRNA expression. Total RNA was extracted from up to 5×10^6 cells, using the QIAshredder spin columns, the RNeasy Mini Kit and the RNase-free DNase Kit (all from Qiagen, Hilden, Germany), according to manufacturers instructions, and specific transcripts were amplified as described in Supplementary material.

Enzymatic assays. Proteolytic activity of *gzmB* using the colorimetric substrate Ac-Ile-Glu-Pro-Asp-pNA (Bachem, Weil am Rhein, Germany) was performed as described previously.¹⁷

Mast cell degranulation assays. BMBC were preloaded overnight with DNP-specific IgE (0.2 μg/ml, clone SPE-7; SIGMA, Deisenhofen, Germany) and subsequently stimulated with antigen (DNP-HSA, containing 30–40 moles DNP per mol albumin, (20 ng/ml; SIGMA, Deisenhofen, Germany) or SCF (100 ng/ml) or a combination of both in RPMI 1640 without phenol red containing 10 mM Hepes (pH 7.4) and 2 mg/ml BSA (10⁶ cells/ml) in duplicates or triplicates for 30 min at 37°C. SN were collected and stored at -80°C until usage for determination of *gzmB* enzymatic activity. The degree of degranulation was determined by measuring the activity of released (sup) and cellular (pel) β-hexosaminidase.⁴⁵ Percentage of degranulation was calculated using the following formula: %degr = [activity(sup)/(activity(sup) + activity(pel))] × 100.

Cell detachment and cytotoxicity induced by recombinant *gzmB* or mast cell supernatants. MEF or MC.Fas^{-/-} cells were plated

(2×10^4 cell/well, triplicates, 96-well plates) and cultured overnight in MEM (+ 5% FCS). Adherent cells were washed with PBS (× 2) and incubated with the indicated amounts of the following preparations: pro-*gzmB*, *gzmB*, SN from mast cells, SLO⁴⁶ or mixtures of SLO and pro-*gzmB* or *gzmB*, for 4 h or 24 h. In some experiments, *gzmB* or mast cell SN were pre-incubated with 100 μM AAD-cmk (Bachem) for 30 min at 37°C to inactivate *gzmB*. Following treatment for 4 h/24 h, survival of MEFs/MC.Fas^{-/-} cells was monitored as described previously.⁴⁷ A similar assay was used for treatment and monitoring non-adherent EL4 cells. For each cell line, sublytic doses of SLO were determined, before further testing.

Immunofluorescence. Cell lines and *ex vivo*-derived LCMV-immune CTL were analyzed by confocal microscopy, as described previously.⁴⁸

bEnd.5 endothelioma cells were grown on LabTek chamber slides (Nalgene-Nunc, Wiesbaden, Germany) and stained as described previously.⁴⁹ Phase contrast microscopy was performed on a Leica DM RXA microscope (Leica Microsystems, Wetzlar Germany). Abs are described in Supplementary material.

BMBC-mediated cytotoxicity. MEFs were added to 96-well plates (2×10^4 cell/well in triplicates) and cultured overnight in MEM (5% FCS). Adherent cells were washed twice with PBS, treated with 100 μl PBS/4 mM DNB-S for 10 min at 37°C, and washed again (2 ×) with MEM (5% FCS), followed by MEM, supplemented with 2 mg/ml BSA and 100 ng/ml SCF. BMBCs, preloaded with mAb IgE (see above) were added to DNB-S-labeled MEFs and incubated for 24 h. Subsequently, SNs were removed and percentages of survival of the attached cells were quantified by ³H-thymidine incorporation and comparison of values to those from proliferation rates of log2 dilutions of the respective cell line as described previously.⁴⁷

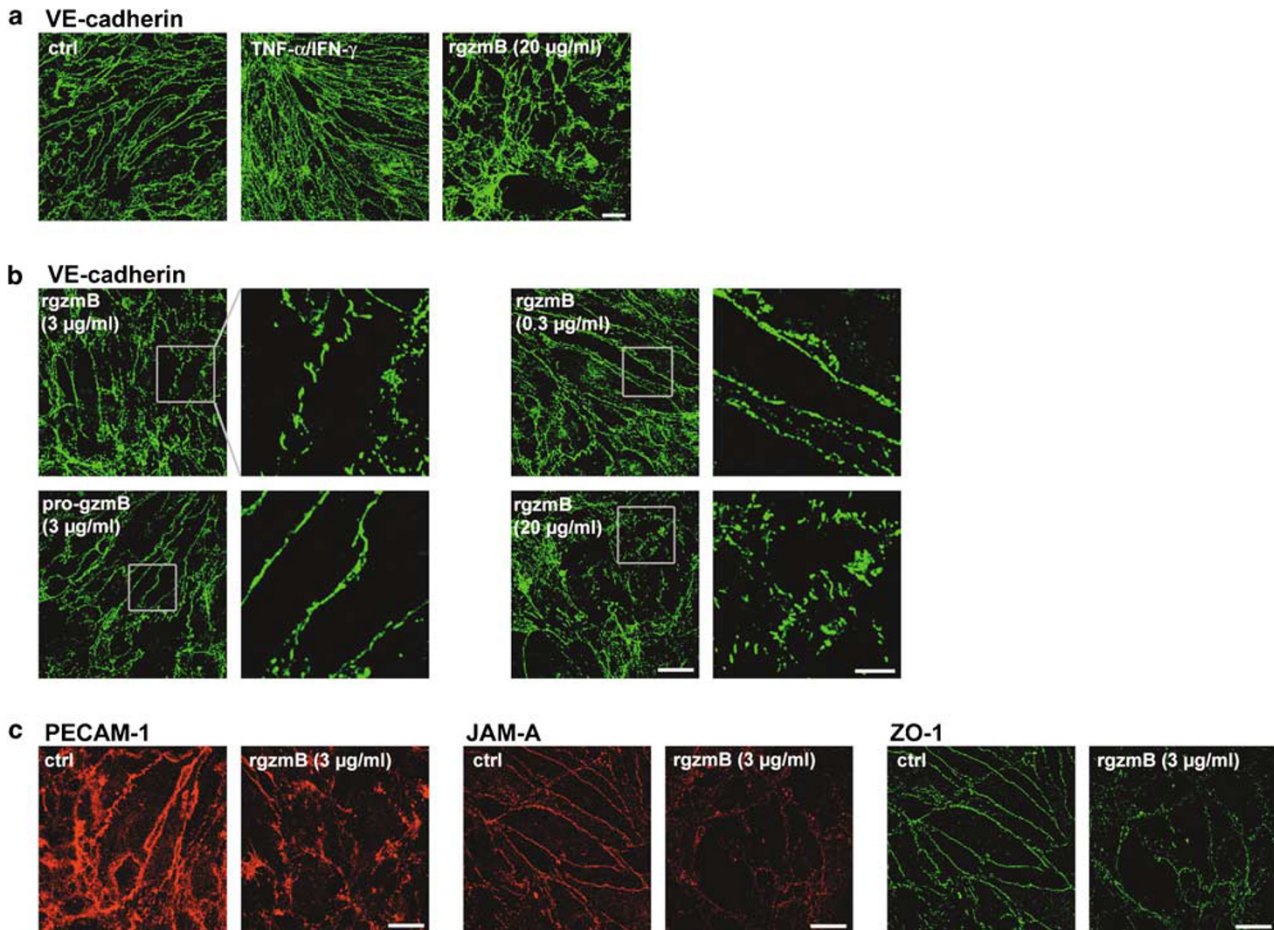


Figure 8 GzmB induces a disorganization of endothelial cell–cell contacts. (a) bEnd.5 EC were treated with 20 $\mu\text{g/ml}$ gzmB for 24 h, then fixed and stained for VE-cadherin. Control cells were either left untreated (ctrl) or incubated with a combination of TNF- α and IFN- γ (1000 U/ml each). Note that gzmB treatment results in multiple gaps in the EC monolayer. Bar, 20 μm . (b) bEnd.5 EC were incubated for 24 h with the indicated concentrations of active gzmB or with 3 $\mu\text{g/ml}$ of inactive gzmB (pro-gzmB) and stained for VE-cadherin. The right panels reflect magnifications of the regions delineated by the gray insets. GzmB treatment disrupts the linear staining pattern of VE-cadherin in a dose-dependent manner. Bars: left panels, 20 μm ; right panels; 5 μm . (c) bEnd.5 EC were incubated with 3 $\mu\text{g/ml}$ gzmB for 24 h and stained with Ab against PECAM-1, JAM-A and ZO-1. GzmB treatment results in a fragmented staining pattern of all three molecules. Bars, 20 μm

For treatment of EL4, 6×10^5 cells were incubated with 500 μl of PBS/4 mM DNB-S for 10 min at 37°C, washed with MEM (5% FCS; $\times 2$) and resuspended in MEM supplemented with 2 mg/ml BSA + 100 ng/ml SCF. A 2×10^4 portion of cells was seeded in 96-well plates (triplicates) and incubated with mAb IgE pre-loaded BMDCs for 24 h. Survival of EL4 cells was quantified by ^3H -thymidine incorporation as described previously.⁴⁷ BMDCs are unable to proliferate in the absence of IL-3.

CTL-mediated cytotoxicity. Plated MC.Fas^{-/-} cells were pretreated with the LCMV-immunodominant peptide gp33 for 2 h before incubation with *ex vivo*-derived LCMV-immune CTLs from B6, perfxgzmA^{-/-} and perfxgzmAxB^{-/-} at indicated effector : target cell ratios for 24 h, as described previously.⁷ Cell survival was quantified by ^3H -thymidine incorporation as described previously.⁴⁷

Histological and immunohistological analysis. Skin and lung tissues from naive C57BL/6 (B6) mice were removed and fixed in phosphate-buffered saline (PBS plus formaldehyde, 4%) before being embedded in paraffin. Sections were stained with alcian blue alone or counterstained with safranin as described previously.¹⁵ Photomicrographs were taken by using a Zeiss microscope provided with an Axiocam camera and Axiovision software.

Alcian blue-stained sections were used for immunostaining for gzmB expression. Accordingly, sections were incubated with 0.6% H₂O₂ (30 min) in methanol to block endogenous peroxidase, followed by treatment (3 h at room temperature) with 5% goat serum in Roti-Block buffer (Roth, Karlsruhe, Germany). Next, consecutive

sections were incubated at 4°C overnight either with rabbit anti-gzmB or -gzmA IgG or with control rabbit IgG (1 : 200 diluted in Roti-Block). After thorough washing, sections were further incubated (2 h at room temperature) with goat anti-rabbit IgG as secondary antibody, labeled with horseradish peroxidase. After washing, slides were incubated (1 h) with diaminobenzidine (Sigma), followed by addition of 0.3% H₂O₂ (15–20 min). Photomicrographs were taken by using a Zeiss microscope provided with an Axiocam camera and Axiovision software.

Acknowledgements. We thank Sucharit Bhakdi for his generous gift of streptolysin. JP was supported by a grant from the Alexander von Humboldt Foundation and AM by a grant from the National Health & Medical Research Council of Australia.

Note added in proof

During the course of the reviewing process, a study appeared demonstrating that human mast cells produce gzmB *in vivo* and *in vitro* and release it upon activation.⁵⁰

1. Metz M, Maurer M (2007) Mast cells – key effector cells in immune responses. *Trends Immunol* 28: 234–241.
2. Marshall JS (2004) Mast-cell responses to pathogens. *Nat Rev Immunol* 4: 787–799.
3. Gall SJ, Nakae S, Tsai M (2005) Mast cells in the development of adaptive immune responses. *Nat Immunol* 6: 135–142.

4. Kataoka TR, Morii E, Oboki K, Kitamura Y (2004) Strain-dependent inhibitory effect of mutant mi-MITF on cytotoxic activities of cultured mast cells and natural killer cells of mice. *Lab Invest* **84**: 376–384.
5. Russell JH, Ley TJ (2002) Lymphocyte-mediated cytotoxicity. *Annu Rev Immunol* **20**: 323–370.
6. Stinchcombe JC, Bossi G, Booth S, Griffiths GM (2001) The immunological synapse of CTL contains a secretory domain and membrane bridges. *Immunity* **15**: 751–761.
7. Pardo J, Bosque A, Brehm R, Wallich R, Naval J, Mullbacher A *et al.* (2004) Apoptotic pathways are selectively activated by granzyme A and/or granzyme B in CTL-mediated target cell lysis. *J Cell Biol* **167**: 457–468.
8. Simon MM, Ebnet K, Kramer MD (1993) Molecular analysis and possible pleiotropic function(s) of the T cell-specific serine proteinase 1. In: Sitkovsky MV, Henkart PA (eds). *Cytotoxic Cells: Recognition, Effector Function, Generation, and Methods*. Birkhäuser: Boston, Basel, Berlin pp 278–294.
9. Suidan HS, Bouvier J, Schaerer E, Stone SR, Monard D, Tschopp J (1994) Granzyme A released upon stimulation of cytotoxic T lymphocytes activates the thrombin receptor on neuronal cells and astrocytes. *Proc Natl Acad Sci USA* **91**: 8112–8116.
10. Buzza MS, Zamurs L, Sun J, Bird CH, Smith AI, Trapani JA *et al.* (2005) Extracellular matrix remodeling by human granzyme B via cleavage of vitronectin, fibronectin, and laminin. *J Biol Chem* **280**: 23549–23558.
11. Choy JC, Hung VH, Hunter AL, Cheung PK, Motyka B, Goping IS *et al.* (2004) Granzyme B induces smooth muscle cell apoptosis in the absence of perforin: involvement of extracellular matrix degradation. *Arterioscler Thromb Vasc Biol* **24**: 2245–2250.
12. Simon MM, Simon HG, Fruth U, Epplen J, Muller-Hermelink HK, Kramer MD (1987) Cloned cytolytic T-effector cells and their malignant variants produce an extracellular matrix degrading trypsin-like serine proteinase. *Immunology* **60**: 219–230.
13. Tak PP, Spaeny-Dekking L, Kraan MC, Breedveld FC, Froelich CJ, Hack CE (1999) The levels of soluble granzyme A and B are elevated in plasma and synovial fluid of patients with rheumatoid arthritis (RA). *Clin Exp Immunol* **116**: 366–370.
14. Froelich CJ, Zhang X, Turbov J, Hudig D, Winkler U, Hanna WL (1993) Human granzyme B degrades aggrecan proteoglycan in matrix synthesized by chondrocytes. *J Immunol* **151**: 7161–7171.
15. Stevens RL, Rothenberg ME, Levi-Schaffer F, Austen KF (1987) Ontogeny of *in vitro*-differentiated mouse mast cells. *Fed Proc* **46**: 1915–1919.
16. Gimborn K, Lessmann E, Kuppig S, Krystal G, Huber M (2005) SHIP down-regulates FcεpsilonR1-induced degranulation at supraoptimal IgE or antigen levels. *J Immunol* **174**: 507–516.
17. Martin P, Wallich R, Pardo J, Mullbacher A, Munder M, Modolell M *et al.* (2005) Quiescent and activated mouse granulocytes do not express granzyme A and B or perforin: similarities or differences with human polymorphonuclear leukocytes? *Blood* **106**: 2871–2878.
18. Chen JW, Pan W, D'Souza MP, August JT (1985) Lysosome-associated membrane proteins: characterization of LAMP-1 of macrophage P388 and mouse embryo 3T3 cultured cells. *Arch Biochem Biophys* **239**: 574–586.
19. Tschopp J, Nabholz M (1990) Perforin-mediated target cell lysis by cytolytic T lymphocytes. *Annu Rev Immunol* **8**: 279–302.
20. Schwartz LB, Austen KF (1980) Enzymes of the mast cell granule. *J Invest Dermatol* **74**: 349–353.
21. Huber M, Helgason CD, Scheid MP, Duronio V, Humphries RK, Krystal G (1998) Targeted disruption of SHIP leads to Steel factor-induced degranulation of mast cells. *EMBO J* **17**: 7311–7319.
22. Rival Y, Del Maschio A, Rabiet MJ, Dejana E, Duperray A (1996) Inhibition of platelet endothelial cell adhesion molecule-1 synthesis and leukocyte transmigration in endothelial cells by the combined action of TNF-alpha and IFN-gamma. *J Immunol* **157**: 1233–1241.
23. Dejana E (2004) Endothelial cell-cell junctions: happy together. *Nat Rev Mol Cell Biol* **5**: 261–270.
24. Raja SM, Metkar SS, Froelich CJ (2003) Cytotoxic granule-mediated apoptosis: unraveling the complex mechanism. *Curr Opin Immunol* **15**: 528–532.
25. Dikov MM, Springman EB, Yeola S, Serafin WE (1994) Processing of procarboxypeptidase A and other zymogens in murine mast cells. *J Biol Chem* **269**: 25897–25904.
26. Salvesen G, Engild JJ (1990) An unusual specificity in the activation of neutrophil serine proteinase zymogens. *Biochemistry* **29**: 5304–5308.
27. Huang C, Friend DS, Qiu WT, Wong GW, Morales G, Hunt J *et al.* (1998) Induction of a selective and persistent extravasation of neutrophils into the peritoneal cavity by tryptase mouse mast cell protease 6. *J Immunol* **160**: 1910–1919.
28. Hallgren J, Spillmann D, Pejler G (2001) Structural requirements and mechanism for heparin-induced activation of a recombinant mouse mast cell tryptase, mouse mast cell protease-6: formation of active tryptase monomers in the presence of low molecular weight heparin. *J Biol Chem* **276**: 42774–42781.
29. Stepp SE, Dufourcq-Lagelouse R, Le Deist F, Bhawan S, Certain S, Mathew PA *et al.* (1999) Perforin gene defects in familial hemophagocytic lymphohistiocytosis. *Science* **286**: 1957–1959.
30. Marshall JS, Jawdat DM (2004) Mast cells in innate immunity. *J Allergy Clin Immunol* **114**: 21–27.
31. Echtenacher B, Mannel DN, Hultner L (1996) Critical protective role of mast cells in a model of acute septic peritonitis. *Nature* **381**: 75–77.
32. Malaviya R, Ikeda T, Ross E, Abraham SN (1996) Mast cell modulation of neutrophil influx and bacterial clearance at sites of infection through TNF-alpha. *Nature* **381**: 77–80.
33. Nourshargh S, Marelli-Berg FM (2005) Transmigration through venular walls: a key regulator of leukocyte phenotype and function. *Trends Immunol* **26**: 157–165.
34. Meredith JR JE, Fazeli B, Schwartz MA (1993) The extracellular matrix as a cell survival factor. *Mol Biol Cell* **4**: 953–961.
35. Wang Y, Jin G, Miao H, Li JY, Usami S, Chien S (2006) Integrins regulate VE-cadherin and catenins: dependence of this regulation on Src, but not on Ras. *Proc Natl Acad Sci USA* **103**: 1774–1779.
36. Choy JC, Cruz RP, Kerjner A, Geisbrecht J, Sawchuk T, Fraser SA *et al.* (2005) Granzyme B induces endothelial cell apoptosis and contributes to the development of transplant vascular disease. *Am J Transplant* **5**: 494–499.
37. Hansson GK, Libby P (2006) The immune response in atherosclerosis: a double-edged sword. *Nat Rev Immunol* **6**: 508–519.
38. Kaartinen M, Penttila A, Kovanen PT (1994) Accumulation of activated mast cells in the shoulder region of human coronary atheroma, the predilection site of atheromatous rupture. *Circulation* **90**: 1669–1678.
39. Choy JC, McDonald PC, Suarez AC, Hung VH, Wilson JE, McManus BM *et al.* (2003) Granzyme B in atherosclerosis and transplant vascular disease: association with cell death and atherosclerotic disease severity. *Mod Pathol* **16**: 460–470.
40. Lu LF, Lind EF, Gondek DC, Bennett KA, Gleeson MW, Pino-Lagos K *et al.* (2006) Mast cells are essential intermediaries in regulatory T-cell tolerance. *Nature* **442**: 997–1002.
41. Kummer JA, Tak PP, Brinkman BM, van Tilborg AA, Kamp AM, Verweij CL *et al.* (1994) Expression of granzymes A and B in synovial tissue from patients with rheumatoid arthritis and osteoarthritis. *Clin Immunol Immunopathol* **73**: 88–95.
42. Kiener HP, Baghestanian M, Dominkus M, Walchshofer S, Ghannadan M, Willheim M *et al.* (1998) Expression of the C5a receptor (CD88) on synovial mast cells in patients with rheumatoid arthritis. *Arthritis Rheum* **41**: 233–245.
43. Lee DM, Friend DS, Gurish MF, Benoist C, Mathis D, Brenner MB (2002) Mast cells: a cellular link between autoantibodies and inflammatory arthritis. *Science* **297**: 1689–1692.
44. Johnston B, Burns AR, Kubes P (1998) A role for mast cells in the development of adjuvant-induced vasculitis and arthritis. *Am J Pathol* **152**: 555–563.
45. Nishizumi H, Yamamoto T (1997) Impaired tyrosine phosphorylation and Ca²⁺ mobilization, but not degranulation, in lyn-deficient bone marrow-derived mast cells. *J Immunol* **158**: 2350–2355.
46. Bhakdi S, Bayley H, Valeva A, Walev I, Walker B, Kehoe M *et al.* (1996) Staphylococcal alpha-toxin, streptolysin-O, and *Escherichia coli* hemolysin: prototypes of pore-forming bacterial cytolytins. *Arch Microbiol* **165**: 73–79.
47. Pardo J, Balkow S, Anel A, Simon MM (2002) Granzymes are essential for natural killer cell-mediated and perfacilitated tumor control. *Eur J Immunol* **32**: 2881–2887.
48. Pardo J, Perez-Galan P, Gamen S, Marzo I, Monleon I, Kaspar AA *et al.* (2001) A role of the mitochondrial apoptosis-inducing factor in granulysin-induced apoptosis. *J Immunol* **167**: 1222–1229.
49. Ebnet K, Suzuki A, Horikoshi Y, Hirose T, Meyer Zu Brickwedde MK, Ohno S *et al.* (2001) The cell polarity protein ASIP/PAR-3 directly associates with junctional adhesion molecule (JAM). *EMBO J* **20**: 3738–3748.
50. Strik MCM, de Koning PJA, Kleijmeer MJ, Bladergroen BA, Wolbink AM, Griffith JM *et al.* Human mast cells produce and release the cytotoxic lymphocyte-associated protease granzyme B upon activation. *Mol Immunol* **2007**; **44**: 3462–3472.

Supplementary Information accompanies the paper on Cell Death and Differentiation website (<http://www.nature.com/cdd>)